Impaired Arginine Metabolism in Hair Follicles: A Potential Mechanism in Androgenetic Alopecia

Ji Li (liji_xy@csu.edu.cn)
Xiangya Hospital, Central South University https://orcid.org/0000-0003-0931-5562

xin duan
Xiangya Hospital, Central South University

fan cheng
Xiangya Hospital, Central South University

guo li
Xiangya Hospital, Central South University

Zhi-Li Deng
Xiangya Hospital, Central South University https://orcid.org/0000-0002-8590-9840

li yang
Xiangya Hospital, Central South University

jin zhang
The Second Hospital of Hunan University of Chinese Medicine

fen liu
Xiangya Hospital, Central South University

yun li
Xiangya Hospital, Central South University

zheng wu
Xiangya Hospital, Central South University

ting chen
Xiangya Hospital, Central South University https://orcid.org/0000-0001-9379-6818

ben wang
Xiangya Hospital, Central South University

xiang zhao
Xiangya Hospital, Central South University

wei shi
Xiangya Hospital, Central South University

fu xie
Xiangya Hospital, Central South University

yan tang
Xiangya Hospital, Central South University

Article

Keywords:

Posted Date: December 19th, 2023

DOI: https://doi.org/10.21203/rs.3.rs-3629594/v1

Additional Declarations: There is **NO** Competing Interest.

Abstract

Androgenetic alopecia (AGA) is a prevalent hair loss disorder characterized by an unclear pathogenesis mechanism and limited therapeutic efficacy. Despite a growing body of evidence indicating a link between AGA and metabolic disorders, the precise role of metabolism in AGA development remains elusive. In this study, we employed targeted metabolome profiling to identify distinct metabolic signatures in AGA patients, with a particular focus on amino acid-related metabolic pathways. Notably, our findings highlight a significant decrease in serum abundance of arginine in AGA patients.Locally, impaired arginine metabolism in hair follicles (HFs) experiencing balding was assumed, as evidenced by the heightened expression of ARG1, the pivotal enzyme regulating the arginine-ornithine transition, and the diminished expression of the arginine transporter SLC7A1. Our study further demonstrated that arginine deficiency hinders human hair growth by antagonizing the mTOR signaling pathway. Moreover, the administration of arginine effectively safeguards against the inhibition of hair growth induced by DHT in an AGA-like mouse model and in balding HFs obtained from AGA patients.Collectively, these findings reveal that obstruction of anagen maintenance cause by arginine deficiency occurs in AGA patients and raise the possibility of supplementation with arginine as a promising clinical treatment strategy.

Introduction

Androgenetic alopecia (AGA) is the predominant form of non-scarring alopecia observed in clinical practice, characterized by the prominent clinical features of a receding hairline, thinning, and sparse hair on the temporal and vertex regions of the scalp[1]. AGA has a considerably high prevalence, reaching up to 74.8% [2,3]. The impact of alopecia on patients' physical and mental well-being, particularly in terms of their social image, necessitates a comprehensive investigation into the underlying mechanisms and the development of targeted therapeutic interventions[4,5].

AGA is featured by the progressive and patterned conversion of large terminal hair follicles (HFs) into intermediate/miniaturized HFs, which is termed as HF miniaturization[6–8]. The current prevailing theories regarding the mechanism of hair miniaturization in AGA suggest that it is a hereditary condition caused by aberrant androgen sensitivity and activity[9,10]. However, the clinical effectiveness of anti-androgen therapy, such as the oral administration of finasteride and spironolactone, is limited, particularly in cases of moderate to severe AGA, coupled with several unexpected side effect[11–13]. Consequently, numerous studies are currently endeavoring to elucidate the potential pathogenic mechanism underlying AGA from alternative viewpoints. Notably, researchers have explored the influence of mechanical stress on AGA and the administration of botulinum toxin, which induces muscle relaxation in the scalp, has been found to effectively stimulate hair growth in individuals with AGA[14]. From the perspective of inflammation, the presence of inflammatory infiltration surrounding the miniaturized hair follicles in AGA specimens, particularly in the isthmus region, was observed and demonstrated a positive correlation with apoptosis[15]. Meanwhile, the oxygen microenvironment may be involved in the pathogenesis of AGA via hypoxia-inducible factor-1 and Wnt/β-catenin signalling pathways [16]. While these factors necessitate

further comprehensive investigation to ascertain their roles in the pathogenesis of AGA, they imply that AGA is a multifactorial disease with potential unidentified pathogenic factors.

Several fundamental investigations have indicated a close association between AGA and various metabolic disorders[17,18]. Patients with AGA have a higher likelihood of presenting with metabolic syndrome, insulin resistance, and type 2 diabetes[19,20]. Early-onset AGA (age < 35 years) may serve as a clinical indicator of insulin resistance[21]. Factors such as waist circumference and blood pressure may play a significant role in the development of female AGA[22]. In addition, a relative nutrient insufficiency and dormant metabolism in intermediate HFs of female pattern hair loss has been reported[23]. Hence, the aforementioned studies indicate that there may be changes in the metabolic status of individuals with AGA, and these alterations could potentially be linked to the development and progression of AGA. However, investigations into the correlation between AGA and metabolic disorders have primarily been confined to clinical observations, with limited exploration in underlying mechanism.

Accumulating evidence suggests that metabolites are important for cell survival and density decision[24–26]. Metabolomics presents a promising avenue for the identification of metabolites that can offer valuable insights into the etiology, treatment, and early detection of diseases. In this article, we presented the previously undisclosed metabolomics alteration in patients with AGA and have elucidated the compromised arginine metabolism in these individuals. Our findings indicated that arginine deficiency of the HFs in the balding region of AGA patients may lead to the inhibition of HF growth and matrix proliferation via inhibition of mTOR signaling pathway. Furthermore, supplementation with arginine has been shown to improve hair growth in AGA-like mice induced by dihydrotestosterone (DHT) and in balding HFs derived from AGA patients. Taken together, our results suggest that incorporating arginine into the diet could offer innovative therapeutic approaches for AGA.

Results

Metabolic alterations are identified in AGA patients compared with healthy controls

In order to examine the potential metabolites implicated in the development of androgenetic alopecia (AGA), a comprehensive analysis of metabolomics was conducted on a cohort of 48 AGA patients and 52 healthy controls matched for sex and age. The quality of the Quality Control (QC) samples was meticulously monitored. A total of 306 metabolites were quantitatively assessed using ultra-performance liquid chromatography coupled to tandem mass spectrometry (UPLC-MS/MS), resulting in the detection of 159 metabolites encompassing Carbohydrates, Amino Acids, Fatty Acids, Organic Acids, and other compounds (Fig. 1A). Principal component analysis (PCA) and orthogonal partial least square discriminant analysis (OPLS-DA) revealed a discernible disparity between the AGA group and the healthy control group (Fig. 1B,C). An examination of the average abundance composition ratio of metabolites exhibited a relative augmentation in organic acid metabolites and a reduction in carbohydrates in the

AGA group in comparison to the healthy controls (Fig. 1D). A total of 82 differentially expressed metabolites (DEMs) were identified, which were primarily derived from the amino acids (24.0%), organic acids (24.0%) and fatty acids (18.5%) (Fig. 1E,F). Random forest variable prediction applied on the DEMs predicted the top 15 potential metabolic related biomarkers for AGA (Fig. 1G).

Arginine metabolism is impaired in AGA patients

Subsequently, we conducted pathway and enrichment analyses to comprehensively investigate the metabolic alterations in patients with AGA. Our findings revealed significant modifications in amino acid metabolism among AGA patients when compared to healthy controls, with particular emphasis on the metabolism of aspartate, arginine, and proline (Fig. 2A,B). Subsequently, we examined the fold change of the amino acids involved in these pathways and observed that the most substantial decrease occurred in arginine (Fig. 2C,D). Furthermore, in an effort to gain insights into the local state of arginine metabolism, we conducted a comparison of the mRNA expression levels of genes related to arginine recycling and transport in balding and non-balding HFs from 6 patients with AGA. The findings revealed an upregulation of the arginine hydrolase *ARG1* in the balding group, indicating an increase in the arginine-ornithine transition, which could be verified by the elevation of ornithine concentration in the AGA patients (Fig. 2D). Additionally, it was observed that the expression of several transporters was downregulated in the balding scalps, as further confirmed by immunofluorescence staining of SLC7A1, the primary arginine transporter (Fig. 2D).These data suggest a possible impairment in arginine uptake within balding hair follicles. In order to confirm this hypothesis, we synthesized arginine coupled with FITC to enhance the visualization of arginine absorption. The results of an ex vivo experiment demonstrated a significant reduction in arginine absorption in balding hair follicles (Fig. 2F). Taken together, these findings provide evidence of arginine deficiency in HFs of individuals with AGA.

Arginine is essential for hair growth

To further verify the role of amino acids in the pathogenesis of AGA, we cultured the HF organ ex vivo in medium supplemented with arginine, alanine, aspartic acid and glutamic acid respectively, and observed the hair growth. Fascinating, while alanine, aspartic acid and glutamic acid had minimal effects on HF growth (Supplementary Fig. 1A), arginine significantly promoted hair growth ex vivo (Fig. 3A-C). Furthermore, we detected the proliferation of hair matrix, the source cells fuel the hair shaft, under the treatments with arginine via KI67 staining. As shown, arginine could promote hair matrix proliferation in a dose dependent manner (Fig. 3D,E). Experiments for arginine depletion in the culture medium were then carried out to determine whether arginine is necessary for HF growth. As expected, arginine deprivation repressed the elongation of HFs significantly, which could be reversed by replenishment of arginine with a dosage dependence (Fig. 3F-G). Interestingly, the morphology of the HFs altered distinctly after depletion of arginine, presenting with a thinning hair shaft/hair matrix right above the hair bulb on day 2. The hair shaft kept narrowing, which developed into a clubbed hair appearance on day 4, leaving with a separated hair bulb and fading melanin granules in the hair shaft on day 6 (Fig. 3H,I). In addition, supplementation with aspartic acid and citrulline, the substrate for arginine synthesis, partially rescued the phenotype induced by arginine deprivation, further demonstrating that arginine is essential for hair follicle growth

and it's not sufficient for the HF cells to synthesis it on their own (Supplementary Fig. 2A-C). Meanwhile, KI67 and pHH3 staining revealed that arginine deprivation significantly decreased proliferating hair matrix cells, which could be rescued by replenishment of arginine (Fig. 3J-L, Supplementary Fig. 2A-C,). Plus, the colony-forming assay revealed an apparent inhibition of arginine deprivation on HaCaT (an epidermal keratinocyte cell line) proliferation (Supplementary Fig. 2G). However, there was little effect of arginine deprivation on hair matrix apoptosis as shown by TUNEL staining (Supplementary Fig. 2D,E).

The dermal papilla (DP) is thought to be the source of signals for the growth and differentiation of surrounding hair matrix cells. Activation of androgen receptor (AR) signaling in DP cells in balding area, which contributes to the regression of blood vessels, is involved in the development of AGA[10]. Interestingly, the activation of AR induced by dihydrotestosterone (DHT) in immortalized DP cells with overexpression of AR led to the downregulation of arginine synthetase ASS1 and the upregulation of arginine hydrolase ARG2, accompanied by a decrease in growth factor production (Supplementary Fig. 3A). This finding suggests a potential insufficiency of arginine in the DP cells of balding HFs. Consequently, we created an arginine-deficient environment by culturing DP cells in a medium with low concentrations of arginine. As a result, the proliferation and growth factor production of DP cells were inhibited in an arginine-deficient state, which could be restored by the replenishment of sufficient arginine (Supplementary Fig. 3B-E).

In order to elucidate the impact of arginine on hair growth, both in vivo and ex vivo, we utilized mouse skin organoids as a model. Intriguingly, our findings revealed that arginine deprivation led to impaired skin formation in the mouse skin organoids. Specifically, the thickness of the organoids exhibited an uneven surface and morphology, with a thicker center and thinner edges following arginine deprivation (Supplementary Fig. 4A). Microscopic analysis further demonstrated that arginine deprivation hindered the formation of K14 + epithelial aggregates and proliferation within the organoids (Supplementary Fig. 4B). However, when the skin organoids were transplanted into nude mice, there was no significant difference observed between the groups with or without arginine deprivation (Supplementary Fig. 4C). This lack of difference may be attributed to a compensatory supplementation of arginine in the nude mice in vivo, as their diet was not deprived of arginine and its precursor amino acids. Overall, these findings indicate that arginine plays a crucial role in hair growth.

Deficiency of arginine attenuates HF growth via counteracting mTOR signaling

In order to further investigate the regulatory function and underlying mechanism of arginine on hair follicles (HFs), we utilized RNA-seq analysis to assess the molecular alterations in HFs after a 12-hour deprivation of arginine, prior to any observable morphological changes. Among the various signals that demonstrated disparities between the control and arginine-deficient groups, the mTOR signaling pathway, a prominent regulator of hair regeneration in mice, emerges as noteworthy (Fig. 5A). As confirmed by the staining for p-S6, the marker of mTOR signal activation, at different time points post arginine deprivation, the hair matrix of HFs cultured in arginine-deficient medium exhibited a significant inhibition of the mTOR

pathway (Fig. 5B,C), exactly similar to the balding HFs of AGA patients (Fig. 5D). Consistently, expression of p-S6 in HaCaT declined with restricted arginine in culture medium (Supplementary Fig. 5A). Wnt/β-catenin signaling pathway is another classical pathway in regulating hair follicle stem cells activation and promoting hair follicle cycle progression. However, β-catenin expression was not affected by arginine deprivation in the HFs (Supplementary Fig. 5B). Subsequently, we administered HFs with rapamycin (RAPA), a classical inhibitor of the mTOR pathway, to observe the hair growth (Fig. 5E-G). The effectiveness of RAPA in suppressing the mTOR signal was confirmed through p-S6 staining (Fig. 5H). Similar to arginine deprivation, the application of RAPA resulted in a statistically significant inhibition of HF growth and matrix proliferation (Fig. 5E-I).

To clarify whether the regulation of arginine on hair growth is dependent on activation of mTOR signaling pathway, we administrated 3-BDO, an activator of mTOR signal, to the HFs cultured in medium with insufficient arginine[27]. First, we investigated the efficacy of 3-BDO at different doses in HaCaT and determined the optimal concentration at 5uM (Supplementary Fig. 5C). In HF organ culture, as expected, application of 3-BDO rescued the hair growth and hair matrix proliferation as well as p-S6 level inhibited by arginine insufficiency (Fig. 6A-E). Considering the possibility of off-target of chemicals, we utilized siRNA to knock down TSC2 expression, the endogenous inhibitor of mTORC1, to activate mTOR signaling[28]. Actually, downregulation of TSC2 via siRNA transfection, which was confirmed by qRT-PCR, western blot and IF staining (Fig. 6I, Supplementary Fig. 5D,E), induced a similar effect with 3-BDO(Fig. 6F-L).

Taken together, these findings suggest that arginine deficiency in AGA patients contributes to the development of AGA through regulation of mTOR pathway .

Arginine exerts beneficial effects in hair growth of DHT-induced AGA-like mice and BD HFs

The aforementioned findings have prompted us to contemplate the potential efficacy of arginine as a therapeutic intervention for AGA. Consequently, we established an AGA mice model by dihydrotestosterone (DHT) as previously described, which significantly impeded hair growth in mice following hair depilation[29] (Fig. 6A). Encouragingly, the administration of arginine as a supplement partially restored hair growth in mice during the initial cycle of hair depilation (Fig. 6A,B). It is worth noting that while subcutaneous injection of DHT resulted in an increase in mice body weight, oral consumption of arginine mitigated this elevation to a certain extent (Supplementary Fig. 6A). Given that the progression of AGA is a protracted and chronic process, a second hair depilation procedure was conducted after all the mice had entered the telogen phase 30 days following the initial depilation. In contrast to the control group, which had already progressed to the late anagen phase on the day5 after the second depilation, the hair follicles (HFs) of the mice treated with dihydrotestosterone (DHT) remained in the telogen or early anagen phase based on morphological observations using HE staining and IF co-staining of Ki67 and p-Cadherin (Fig. 6C, Supplementary Fig. 6B,C). Additionally, the level of p-S6 was also suppressed by DHT (Fig. 6D, Supplementary Fig. 6D). However, the replenishment of arginine

has the potential to reverse the retardation of the telogen-anagen transition and the inhibition of the mTOR signal induced by DHT, as illustrated in Fig. 6C and 6D. Furthermore, arginine demonstrates a significant ability to restore the growth of balding hair follicles (HFs) in AGA patients treated with DHT, as depicted in Fig. 6E and 6F. In conclusion, these findings strongly indicate that arginine holds promise as a therapeutic strategy for AGA.

Discussion

Metabolic reprogramming occurs as a hallmark of various disease[25,30–32]. In recent years, significant efforts have been dedicated to elucidating the pathogenesis of AGA, including its metabolic factors[18,20,33]. However, there is still a lack of direct evidence regarding the association between AGA and metabolic disorders. In this study, we have provided a comprehensive analysis of the metabolic changes observed in the serum of patients with AGA compared to healthy controls and highlighted the significance of arginine as a key metabolite in the regulation of hair matrix proliferation and hair growth. Consequently, supplementation with arginine holds promise as a potential therapeutic approach for AGA.

In mice, hair follicle stem cells (HFSCs), which possess the ability to give rise to all HF components, exhibit distinct metabolic pathway preferences, favoring glycolytic metabolism and generating higher levels of lactate compared to other cells in the epidermis[34]. During hair cycle, HFSCs are metabolically flexible to achieve the transition to ORS progenitor cells which requires the activation of OXPHOS and flux of glutamine into TCA cycle[35]. Yet little is known about the metabolic status of human HFs and its role in the pathogenesis of hair loss disorder. In the present study, we has confirmed significant alterations in amino acid metabolism, lipid metabolism and energy metabolism in serum of patients with AGA.

In recent years, there has been significant progress in understanding the prevalence of alterations in the arginine-synthesizing urea cycle in cancer and immune-related diseases[36–40]. Our observations indicate a notable decrease in arginine levels and a corresponding increase in ornithine levels in the serum of patients with AGA, suggesting a heightened metabolic transition from arginine to ornithine in these individuals. This finding is further supported by the upregulation of the key enzyme ARG1 in balding hair follicles. Additionally, previous research has demonstrated the ability of hair follicles in female pattern hair loss (FPHL) to uptake nutrients such as glutamic acid and cystine[23]. However, our research reveals a notable decrease in arginine uptake in HFs obtained from the balding scalp of patients with AGA. This decrease can be attributed to the downregulation of the primary arginine transporter, SLC7A1[39]. Consequently, we propose that balding HFs may experience a deficiency in arginine, which warrants further investigation through local metabolic analysis in future studies. Arginine plays a crucial role in cellular activation, proliferation, and survival[41–43]. Our findings indicate that arginine is indispensable for the ex vivo growth of human HFs, as it sustains and enhances hair matrix proliferation. The premature termination of anagen, leading to hair miniaturization in balding scalps, may be partially explained by the obstruction of matrix proliferation caused by arginine deficiency in HFs.

The dermal papilla (DP) acts as a crucial signal center in promoting HF growth by secreting various growth factors[44,45]. The development of AGA involves AR-mediated vascular regression in DP cells[10]. In this study, we hypothesized that the overexpression of AR leads to a compromised arginine metabolism in DP cells. This hypothesis is supported by the observed downregulation of ASS1, which suppresses arginine synthesis, and the upregulation of ARG2, which promotes the conversion of arginine to ornithine[46,47]. Furthermore, since DP cells primarily rely on nutrient uptake from surrounding blood vessels, the vascular regression in balding HFs may exacerbate the decrease in exogenous arginine import to DP cells. Consequently, the inadequate presence of arginine in DP cells hinders their proliferation and the production of growth factors, thereby impairing their ability to induce the proliferation of hair follicle epithelium cells and impeding hair growth.

The deprivation of arginine regulates cell proliferation via various nutrient sensing pathways[37,39,48]. Our discovery that arginine facilitates the proliferation of the hair matrix and, consequently, hair growth by modulating mTOR signaling bears resemblance to observations made in cancer cells. Although the promotion effect of the mTOR signaling pathway on the activation of HFSCs in mice has received significant attention[49,50], its role in human HFs remains poorly understood. Our study revealed that the mTOR signaling pathway is primarily activated in hair matrix and inner root sheath (IRS) cells in human HFs. Of note, this activation is inhibited in balding HFs of patients with AGA and by arginine deprivation, which could lead to compromised hair growth and involved in the development of AGA.

Can arginine's role in promoting hair growth be exploited for AGA therapy? It has been found that the combination of inositol-stabilized arginine silicate complex and biomagnesium can promote the regeneration of mouse nails and hair, but in this study, the use of arginine alone did not promote hair regeneration[51]. In our preliminary exploration, the addition of arginine as a supplement demonstrated a positive impact on hair growth in balding HFs from AGA patients. Interestingly, in addition to promoting hair growth, dietary supplementation with arginine also provided protection against DHT-induced obesity in mice, suggesting a potential role for arginine in addressing metabolic disorders associated with AGA. Furthermore, despite the absence of a primary arginine transporter in balding hair follicles, the application of exogenous arginine over an extended period still exhibited the ability to promote hair growth ex vivo. This could be attributed to the presence of alternative arginine transporters.

Overall, our research findings indicate that a deficiency in arginine hampers hair growth by affecting mTOR signaling and plays a role in the development of AGA. Further investigations are necessary to explore the local metabolic analysis of HFs and identify the specific targets of arginine metabolism, in order to ascertain the exact mechanisms involved. Additionally, while arginine shows promise as a novel therapeutic approach for AGA, its efficacy in promoting hair growth in humans through clinical trials still requires verification.

Materials and Methods

Patient information and sample collection

Participants included in this study were AGA patients aged 18–55, and were first diagnosed by two dermatologists from the Department of Dermatology of Xiangya Hospital from November 2019 to January 2021. The study protocol was approved by the Ethics Committee of Xiangya Hospital, Central South University. Exclusion criteria include: 1) Patients were not first diagnosed in Xiangya Hospital; 2) Patients with other non-scarring alopecia: telogen alopecia, alopecia areata ; 3) Patients with a long medication history of AGA drugs (oral administration of antiandrogen drugs or topical application of minoxidil) and other drugs (corticosteroids, antihypertensive drugs, hypoglycemic drugs, etc.); 4) Patients refused peripheral blood collection. At the same time, healthy control (HC) with age, gender, health status and BMI matched with AGA patients were collected and the exclusion criteria of HC were as follows: 1) Long-term medication history of glucocorticoid, antihypertensive drugs, hypoglycemic drugs, etc.; 2) People combined with other systemic diseases; 3) Patients refused peripheral blood collection.

Targeted metabolomics sequencing and analysis

About 5ml peripheral blood from the median cubital vein of subjects was collected. Serum of the blood was separated and then analyzed by Q300 Kit (Metabo-Profile, China) as previously described[52]. We used ultra-performance liquid chromatography coupled to tandem mass spectrometry (UPLC-MS/MS) system (ACQUITY UPLC-Xevo TQ-S, Waters Corp., Milford, MA, USA) to quantitatively analyze metabolites in the serum of AGA patients and HC. To evaluate stability of the experiment and the reliability of sample source, all the tested samples were mixed to obtain quality control (QC) samples. One QC sample was tested every 10 samples during liquid phase mass spectrometry analysis. MassLynx software (v4.1, Waters, Milford, MA, USA) was used to process raw data files generated by UPLC-MS / MS. IMAP (v1.0; metabo-Profile, China) platform was used to statistically analyzed peak integration, calibration and quantification of each metabolite.

Human hair follicle organ culture

The informed consent of AGA patients was obtained before sample collection. During hair transplantation surgery, hair follicle units from scalp of AGA patients were collected and carefully isolated under the stereo microscope. Then, the isolated hair follicles with a complete physiological structure (including dermal papilla and continuous dermal sheath) were cultured in 24-well dishes for 6–8 days in William's E medium (Gibco, USA) supplemented with 10 mg/mL insulin, 2 mM L-glutamine, 10 ng/mL hydrocortisone, and 100 U/mL penicillin-streptomycin at 37°C in a 5% (v/v) CO2 atmosphere. DMEM for SILAC (Thermo Scientific™, USA) lacked L-arginine, L-leucine and L-lysine and was used to replace William's E medium after adding 84mg/ml L-Arginine hydrochloride, 105mg/ml L-leucine or 146mg/ml L-lysine hydrochloride. By supplementing two of the three amino acids, deprivation of the remaining amino acid was achieved. Hair follicles were photographed by Leica optical microscope at a same time point every 2 days and ImageJ software was used to calculate the growth length and diameter of each hair follicle.

Immunofluorescence(IF) and TUNEL staining

Mouse skin tissue samples were harvested from mid-dorsal areas and fixed, paraffin-embedded, and cut into 5μm sections. The sections were stained with hematoxylin and eosin (H&E) and evaluated using light microscopy (OLYMPUS, Japan). Human hair follicles were embedded in O.C.T. (Tissue Tek), and cut into 6 μm sections. For immunofluorescence, paraffin sections was deparaffinized and rehydrated and were stained with primary antibodies after antigen retrieval. The frozen sections of hair follicles were fixed with 4% paraformaldehyde, blocked with 5% donkey serum at room temperature for 1h, and then incubated with primary antibodies at 4°C overnight. Alexa Fluor 488- or 594-coupled secondary antibodies (Thermo Fisher Scientific, USA) was incubated at room temperature for 1h, and 4',6-diamidino-2-phenylindole (DAPI) was used for nuclear staining. TUNEL staining was performed according to the instruction of TUNEL assay kit (Roche, Switzerland). Photographs were captured by fluorescence microscope. Antibodys and dilution ratio are listed in Table 1.

RNA extraction, real-time PCR (qPCR) and RNAseq

RNA was extracted from cells and human hair follicles using TRIzol Reagent (Thermo Fisher Scientific, USA) and was reverse-transcribed to cDNA by PrimeScript™ RT reagent Kit with gDNA Eraser (Takara, China). qPCR was performed on an Applied Biosystems 7500 machine (Life Technologies) with the program setted up according to the instruction of ChamQ Universal SYBR qPCR Master Mix (Vazyme, China). The relative gene expression was measured by delta-delta CT relative to GAPDH, and the fold change was normalized to the control group. The primer sequences used in this study are listed in Table 2. For RNAseq, transcriptome sequencing was performed using Illumina HiSeq X Ten (Novogene, China). Differentially expressed genes (DEGs) were identified with $|logFC| > 0.5$ and adjust. $p < 0.05$, using the DESeq R package. GO and KEGG enrichment analyses were performed using “clusterProfiler,” “enrichplot,” and “ggplot2” R packages. The PPI network was used for hub gene analysis using STRING (https://cn.string-db.org/) and Cytoscape (version 3.8.2).

Immunoblotting

Cells were lysed in RIPA buffer (Thermo Fisher Scientific, USA) containing protease inhibitors (Thermo Fisher Scientific, USA) after washed with cold PBS. The proteins were quantified via bicinchoninic acid assay (Thermo Fisher Scientific, USA) and separated on SDS-PAGE and transferred to a PVDF membrane. The membrane was blocked with 5% nonfat milk for 1h at room temperature and incubated with primary antibodies overnight at 4℃. The secondary antibodies HRP-conjugated Goat anti-Mouse IgG (Santa Cruz Biotechnology, USA) and HRP-conjugated Goat anti-Rabbit IgG secondary antibody (Santa Cruz Biotechnology, USA) were incubated for 1h at room temperature. The immunoreactive bands were visualized by the HRP substrate (Sigma, USA) on ChemiDoc XRS + system (Bio-Rad). Data were analyzed by GE Healthcare (now Cytiva) ImageQuant LAS 4000 Mini and images have been cropped for presentation. The primary antibodies in this study were listed at Table 1.

RNA interference

Small interferring RNA (siRNA) were purchased from GenePharma (China). The sequences for siTSC2 are listed in Table 2. HaCaT cells were transfected with siRNA at 0.06 nM packaged by Lipofectamine

3000(Invitrogen, Carlsbad, CA, USA) in 6-well plates (5 × 105cells/well). Hair follicles were transfected with siRNA at 0.06 nM packaged by Lipofectamine 3000(Invitrogen, USA) in 24-well plates (1 hair follicle/well).

Cell culture and treatment

The HaCaT keratinocyte cell line was obtained from the NTCC (Laboratory of Biological Carrier Science, China) and immortalized DP cell line(iDP), iDP-AR (AR-overexpressing iDP) cells and iDP-V (vector-overexpressing iDP) cells were generated as previously described(Deng, Chen et al. 2022). Cells cultured in Dulbecco's Modified Eagle's Medium (DMEM, Gibco, USA) containing 10% fetal bovine serum(Gibco, USA) at 37°C and 5% CO2. Before qPCR, iDP-V and iDP-AR cells were treated with 1μM DHT(Selleck, China) for 24h and iDP cells were treated with different concentrations of arginine compared with DMEM for 24h. To analyze the relationship between arginine and HaCaT cells proliferation ability, equal numbers of HaCaT cells (10,000) were plated in 12-well plates and cultured in DMEM or the medium treated with arginine deprivated with or without 0.5mM arginine replenishment. After four days of cultivation, the HaCaT cells were fixed and stained with crystal violet (0.5% wt/vol) and photographed by Leica optical microscope. To figure out whether iDP cells regulate the mTOR pathway activation of HaCaT cells, the conditional medium(CM) was collected from iDP-V or iDP-AR cells and incubated with HaCaT cells for 24h.

CCK8 assay

iDP cells were seeded in 96-well plates at a density of 3 × 103 per well. The cells were treated with 0.05mM and 0.5mM arginine and DMEM. CCK8 reagent was added in each well at different time points and cells were incubated at 37°C for 1h. The optical density (OD) was measured at 450 nm using a microplate reader(Tecan, Switzerland) to calculate the relative viable cells.

EdU proliferation assay

Cell proliferation was assessed using EdU Cell Proliferation Assay kit (RiboBio, China). After 0.05mM and 0.5mM arginine and DMEM treatments, iDP cells were incubated in medium containing 10 μM EdU for 24 hours. Cells were fixed with 4% paraformaldehyde and cell nuclei were stained with DAPI. The proportion of the cells incorporating EdU was determined with fluorescence microscopy.

Visualization of the uptake of FITC-Arginine in human hair follicle

To visualize the uptake of FITC-Arginine(Ruixi Biology, China), hair follicles from both balding and nonbalding scalps of AGA patients were digested in 0.1% dispase(Sigma, USA) at 37℃ for 1h and then, the dermal sheath was removed. The remaining hair follicles were cultured in 24-well dishes treated with 0.5mM FITC-Arg for 4h. Cultivated hair follicles were cut into frozen sections to visualize arginine uptake under a fluorescence microscopy.

Mouse skin organoid culture

Mouse skin organoid model was made according to the previous article[53]. Neonatal mice born within 24 hours were selected and sacrificed by cervical dislocation. The back skin was cut off and digested with 0.1% trypsin at 4°C overnight. On the second day, the epidermis and dermis were isolated and cut into pieces. The dermis tissue was digested with collagenase at 37°C for 30 minutes, and then the epidermis and dermis tissue suspension were filtered separately with a 70μm filter, and centrifuged at 1100rpm/min at room temperature for 15 minutes to obtain epidermal and dermal cells of mouse skin. Then the cells from epidermis and dermis were mixed together and inoculated into a 12-well plate containing a transwell chamber, and the medium was changed for observation for 1–2 days.

Animal treatment

Seven-week-old female C57BL/6 mice were purchased from Slack Company (China). During experiments, the mice were maintained under specific-pathogen-free conditions and were fed normal water or water containing 7 mg/ml L-arginine(Hou, Dong et al. 2020). In catagen, hair shaft was removed from back of the mice with depilatory cream(Weiting, China). 100μl 0.625mg/ml DHT(Sigma, USA) or equivalent vehicle (5.2% PEG300 and 5.2% Tween 80 in 0.9% NaCl) was subcutaneously injected to the depilated area once a day. Hair coat recovery was photographed every two days and was valued based on skin pigmentation levels and hair shaft density[54]. All experiments were approved by the Ethics Committee of Xiangya Hospital, Central South University, Hunan Province, China (IRB number 201611610). All animal experiments comply the National Research Council's Guide for the Care and Use of Laboratory Animals.

Statistical analysis

The metabolite data obtained in our experiment were analyzed by iMAP platform. Statistical analysis methods include: 1) Multivariate statistical analysis: principal component analysis (PCA), partial least squares discriminant analysis (PLS-DA), orthogonal partial least squares discriminant analysis (OPLS-DA), random forest method. 2) Univariate statistical analysis, including t-test, Mann-Whitney-Wilcoxon analysis (u-test), analysis of variance, correlation analysis, etc. The volcanic map threshold of one-dimensional analysis is set as follows: p 0.05; Log2FC > 0 (FC, Fold Change, the fold change between groups). All data were expressed as mean ± SEM and were analyzed by ANOVA or Kruskall-Wallis test when more than two groups were compared or Student's t-test when only two groups were compared. Graphpad Prism 8, R (v4.1.3) and Excel (Microsoft) were used to assess statistical significance. Statistical significance was set at a $P < 0.05$. *, ** and *** indicate $P < 0.05$, $P < 0.01$ and $P < 0.001$, respectively.

Reagents

L-glutamine (Gibco, USA), penicillin-streptomycin (Gibco, USA), insulin (Sigma, USA) hydrocortisone (Selleck, China), L-arginine (Sangon Biotech, China , Aspartic acid (Sigma, USA), citrulline (Sigma, USA), glutamic acid (Sigma, USA), alanine (Sigma, USA), L-leucine (Sigma, USA), L-lysine hydrochloride (Sangon Biotech, China , 3BDO Selleck, China , rapamycin (Selleck, China).

Declarations

Data availability

All data needed to assess the conclusions in the present study are provided in the manuscript and/or the Supplementary Materials. Any other data supporting the findings of this study are available from the corresponding author upon reasonable request.

Acknowledgements

This work was supported by the National Key Research and Development Program of China (No. 2021YFF1201205), the National Natural Science Funds for Distinguished Young Scholars (No. 82225039), the National Natural Science Foundation of China (No. 82373510,No. 82304057, No. 81874251, No. 82073457, No. 82173448, No. 82373508, No. 82303992), the Natural Science Foundation of Hunan Province, China (No. 2020JJ5888), the Natural Science Funds of Hunan province for excellent Young Scholars (No. 2023JJ20094). We thank our colleagues (Department of Dermatology, Xiangya Hospital, Central South University, China) for their generous support throughout this work.

Author contributions

J.L., G.L. and Y.T. designed and conceived the study. Y.T., G.L. and L.Y. performed data analyses. S.D., Y.C., and G.L. performed most experiments. Y.Z., F.L., B.W., Z.Z. and W.S. contributed to sample collection. Z.D. and M.C. help to generate sequencing libraries. H.X. and Z.W. provide critical discussion and suggestion. G.L., Y.C., Y.T. and J.L. prepared the manuscript with input from coauthors.

Competing interests

The authors declare no competing interests.

References

1. Walter, K. Common Causes of Hair Loss. *JAMA* **328**, 686 (2022).
2. Gao, J. L. *et al.* Androgenetic alopecia incidence in transgender and gender diverse populations: A retrospective comparative cohort study. *J Am Acad Dermatol* **89**, 504–510 (2023).
3. Severi, G. *et al.* Androgenetic alopecia in men aged 40-69 years: prevalence and risk factors. *Br J Dermatol* **149**, 1207–1213 (2003).
4. Sinclair, R. Male pattern androgenetic alopecia. *BMJ* **317**, 865–869 (1998).
5. Toussi, A., Barton, V. R., Le, S. T., Agbai, O. N. & Kiuru, M. Psychosocial and psychiatric comorbidities and health-related quality of life in alopecia areata: A systematic review. *J Am Acad Dermatol* **85**, 162–175 (2021).
6. Castro, A. R., Portinha, C. & Logarinho, E. The booming business of hair loss. *Trends Biotechnol* **41**, 731–735 (2023).

7. Chew, E. G. Y. Regulatory pathways implicated in male androgenetic alopecia pathogenesis. *Br J Dermatol* **177**, 1159–1160 (2017).
8. Bienenfeld, A. *et al.* Androgens in women: Androgen-mediated skin disease and patient evaluation. *J Am Acad Dermatol* **80**, 1497–1506 (2019).
9. Liu, F. *et al.* Prediction of male-pattern baldness from genotypes. *Eur J Hum Genet* **24**, 895–902 (2016).
10. Deng, Z. *et al.* Androgen Receptor-Mediated Paracrine Signaling Induces Regression of Blood Vessels in the Dermal Papilla in Androgenetic Alopecia. *J Invest Dermatol* **142**, 2088-2099.e9 (2022).
11. Adil, A. & Godwin, M. The effectiveness of treatments for androgenetic alopecia: A systematic review and meta-analysis. *J Am Acad Dermatol* **77**, 136-141.e5 (2017).
12. Devjani, S., Ezemma, O., Kelley, K. J., Stratton, E. & Senna, M. Androgenetic Alopecia: Therapy Update. *Drugs* **83**, 701–715 (2023).
13. Garcia-Argibay, M., Hiyoshi, A., Fall, K. & Montgomery, S. Association of 5α-Reductase Inhibitors With Dementia, Depression, and Suicide. *JAMA Netw Open* **5**, e2248135 (2022).
14. Shon, U., Kim, M. H., Lee, D. Y., Kim, S. H. & Park, B. C. The effect of intradermal botulinum toxin on androgenetic alopecia and its possible mechanism. *J Am Acad Dermatol* **83**, 1838–1839 (2020).
15. Heymann, W. R. The inflammatory component of androgenetic alopecia. *J Am Acad Dermatol* **86**, 301–302 (2022).
16. Liu, Q. *et al.* Insights into male androgenetic alopecia using comparative transcriptome profiling: hypoxia-inducible factor-1 and Wnt/β-catenin signalling pathways. *Br J Dermatol* **187**, 936–947 (2022).
17. Hair, hormones, and high-risk prostate cancer - PubMed. https://pubmed.ncbi.nlm.nih.gov/25547509/.
18. Sanke, S., Chander, R., Jain, A., Garg, T. & Yadav, P. A Comparison of the Hormonal Profile of Early Androgenetic Alopecia in Men With the Phenotypic Equivalent of Polycystic Ovarian Syndrome in Women. *JAMA Dermatol* **152**, 986–991 (2016).
19. Anderson, B. J. *et al.* Plasma metabolomics supports non-fasted sampling for metabolic profiling across a spectrum of glucose tolerance in the Nile rat model for type 2 diabetes. *Lab Anim* **52**, 269–277 (2023).
20. Association of androgenetic alopecia with mortality from diabetes mellitus and heart disease - PubMed. https://pubmed.ncbi.nlm.nih.gov/23677087/.
21. Matilainen, V., Koskela, P. & Keinänen-Kiukaanniemi, S. Early androgenetic alopecia as a marker of insulin resistance. *Lancet* **356**, 1165–1166 (2000).
22. Yi, S. M. *et al.* Gender-specific association of androgenetic alopecia with metabolic syndrome in a middle-aged Korean population. *Br J Dermatol* **167**, 306–313 (2012).
23. Piccini, I. *et al.* Intermediate Hair Follicles from Patients with Female Pattern Hair Loss Are Associated with Nutrient Insufficiency and a Quiescent Metabolic Phenotype. *Nutrients* **14**, 3357

(2022).

24. Liu, T. *et al.* Aberrant amino acid metabolism promotes neurovascular reactivity in rosacea. *JCI Insight* **7**, e161870 (2022).
25. Shao, Y. *et al.* Comprehensive metabolic profiling of Parkinson's disease by liquid chromatography-mass spectrometry. *Mol Neurodegener* **16**, 4 (2021).
26. J, L. *et al.* Integrative metabolomic characterisation identifies altered portal vein serum metabolome contributing to human hepatocellular carcinoma. *Gut* **71**, (2022).
27. Rheb1 promotes tumor progression through mTORC1 in MLL-AF9-initiated murine acute myeloid leukemia - PubMed. https://pubmed.ncbi.nlm.nih.gov/27071307/.
28. Inoki, K., Li, Y., Xu, T. & Guan, K.-L. Rheb GTPase is a direct target of TSC2 GAP activity and regulates mTOR signaling. *Genes Dev* **17**, 1829–1834 (2003).
29. Fu, D. *et al.* Dihydrotestosterone-induced hair regrowth inhibition by activating androgen receptor in C57BL6 mice simulates androgenetic alopecia. *Biomed Pharmacother* **137**, 111247 (2021).
30. Ortmayr, K., Dubuis, S. & Zampieri, M. Metabolic profiling of cancer cells reveals genome-wide crosstalk between transcriptional regulators and metabolism. *Nat Commun* **10**, 1841 (2019).
31. Chen, C. *et al.* Metabolomic profiling reveals amino acid and carnitine alterations as metabolic signatures in psoriasis. *Theranostics* **11**, 754–767 (2021).
32. Ni, Y., Xie, G. & Jia, W. Metabonomics of human colorectal cancer: new approaches for early diagnosis and biomarker discovery. *J Proteome Res* **13**, 3857–3870 (2014).
33. Miranda, J. J., Taype-Rondan, A., Tapia, J. C., Gastanadui-Gonzalez, M. G. & Roman-Carpio, R. Hair follicle characteristics as early marker of Type 2 Diabetes. *Med Hypotheses* **95**, 39–44 (2016).
34. Flores, A. *et al.* Lactate dehydrogenase activity drives hair follicle stem cell activation. *Nat Cell Biol* **19**, 1017–1026 (2017).
35. Kim, C. S. *et al.* Glutamine Metabolism Controls Stem Cell Fate Reversibility and Long-Term Maintenance in the Hair Follicle. *Cell Metab* **32**, 629-642.e8 (2020).
36. Wu, M., Xiao, H., Shao, F., Tan, B. & Hu, S. Arginine accelerates intestinal health through cytokines and intestinal microbiota. *Int Immunopharmacol* **81**, 106029 (2020).
37. Chen, C.-L. *et al.* Arginine is an epigenetic regulator targeting TEAD4 to modulate OXPHOS in prostate cancer cells. *Nat Commun* **12**, 2398 (2021).
38. Mossmann, D. *et al.* Arginine reprograms metabolism in liver cancer via RBM39. *Cell* **186**, 5068-5083.e23 (2023).
39. Missiaen, R. *et al.* cGCN2 inhibition sensitizes arginine deprived hepatocellular carcinoma cells to senolytic treatment. *Cell Metab* **34**, 1151-1167.e7 (2022).
40. Brunner, J. S. *et al.* Environmental arginine controls multinuclear giant cell metabolism and formation. *Nat Commun* **11**, 431 (2020).
41. Geiger, R. *et al.* L-Arginine Modulates T Cell Metabolism and Enhances Survival and Anti-tumor Activity. *Cell* **167**, 829-842.e13 (2016).

42. Poillet-Perez, L. *et al.* Autophagy maintains tumour growth through circulating arginine. *Nature* **563**, 569–573 (2018).
43. Mussai, F. *et al.* Arginine dependence of acute myeloid leukemia blast proliferation: a novel therapeutic target. *Blood* **125**, 2386–2396 (2015).
44. Morgan, B. A. The dermal papilla: an instructive niche for epithelial stem and progenitor cells in development and regeneration of the hair follicle. *Cold Spring Harb Perspect Med* **4**, a015180 (2014).
45. Liu, Y. *et al.* Hedgehog signaling reprograms hair follicle niche fibroblasts to a hyper-activated state. *Dev Cell* **57**, 1758-1775.e7 (2022).
46. Burki, T. K. Arginine deprivation for ASS1-deficient mesothelioma. *Lancet Oncol* **17**, e423 (2016).
47. Critical role for arginase II in osteoarthritis pathogenesis - PubMed. https://pubmed.ncbi.nlm.nih.gov/30610061/.
48. Chantranupong, L. *et al.* The CASTOR Proteins Are Arginine Sensors for the mTORC1 Pathway. *Cell* **165**, 153–164 (2016).
49. Laplante, M. & Sabatini, D. M. mTOR signaling in growth control and disease. *Cell* **149**, 274–293 (2012).
50. Deng, Z. *et al.* mTOR signaling promotes stem cell activation via counterbalancing BMP-mediated suppression during hair regeneration. *J Mol Cell Biol* **7**, 62–72 (2015).
51. Demir, B. *et al.* Effects of a Combination of Arginine Silicate Inositol Complex and a Novel Form of Biotin on Hair and Nail Growth in a Rodent Model. *Biol Trace Elem Res* **201**, 751–765 (2023).
52. Jia, H. *et al.* Metabolomic analyses reveal new stage-specific features of COVID-19. *Eur Respir J* **59**, 2100284 (2022).
53. Wang, M. *et al.* Mechanical force drives the initial mesenchymal-epithelial interaction during skin organoid development. *Theranostics* **13**, 2930–2945 (2023).
54. Chai, M. *et al.* Stimulation of Hair Growth by Small Molecules that Activate Autophagy. *Cell Rep* **27**, 3413-3421.e3 (2019).

Tables

Table 1
qPCR primers and siRNA sequences

Gene	Forward	Reverse
h-ASS1	TTGAAATTTGCTGAGCTGGTGTA	AGCCTGAGGGAATTGATGTTGAT
h-ASL	GCCGAGATGGACCAGATACTC	CTGCCGTTGCACCAATGAG
h-ARG1	GTGGAAACTTGCATGGACAAC	AATCCTGGCACATCGGGAATC
h-ARG2	ACCTGATAGTGAATCCACGCT	CATGGGCATCAACCCAGAC
h-SLC7A1	GCCTGTGCTATGGCGAGTTT	ACGCTTGAAGTACCGATGATGTA
h-SLC7A5	CCGTGAACTGCTACAGCGT	CTTCCCGATCTGGACGAAGC
h-SLC7A8	AGGCTGGAACTTTCTGAATTACG	ACATAAGCGACATTGGCAAAGA
h-SLC7A11	TGTGTGGGGTCCTGTCACTA	CAGTAGCTGCAGGGCGTATT
h-KGF	AATTCCAACTGCCACTGTCC	GACATGGATCCTGCCAACTT
h-VEGF	GCGAGTCTGTGTTTTTGCAG	TCTTCAAGCCATCCTGCGTG
h-AR	CCAGGGACCATGTTTTGCC	CGAAGACGACAAGATGGACAA
h-WNT5A	ATTCTTGGTGGTCGCTAGGTA	CGCCTTCTCCGATGTACTGC
h-GAPDH	TGTTGCCATCAATGACCCCTT	CTCCACGACGTACTCAGCG
h-TSC2	GGCAAGAGAGTAGAGAGGGACG	AAGAAGGGGGAATGGTAGAGC
siTSC2-1	CAATGAGTCACAGTCCTTTGA	TCAAAGGACTGTGACTCATTG
siTSC2-2	AAGGATTACCCTTCCAACGAA	TTCGTTGGAAGGGTAATCCTT

Table 2
Antibodies used in this study

Antibody	Supplier	IB conditions	IF conditions
SLC7A1	Atlas Antibodies		1:100
Ki67	Thermo Scientific		1:500
PHH3	Abcam		1:500
K14	Abcam		1:200
Vim	Cell Signaling		1:100
pS6	Cell Signaling	1:5000	1:1000
S6	Cell Signaling	1:2000	
K15	Thermo Scientific		1:500
β-catenin	Cell Signaling	1:1000	1:100
GAPDH	Cell Signaling	1:10000	

Figures

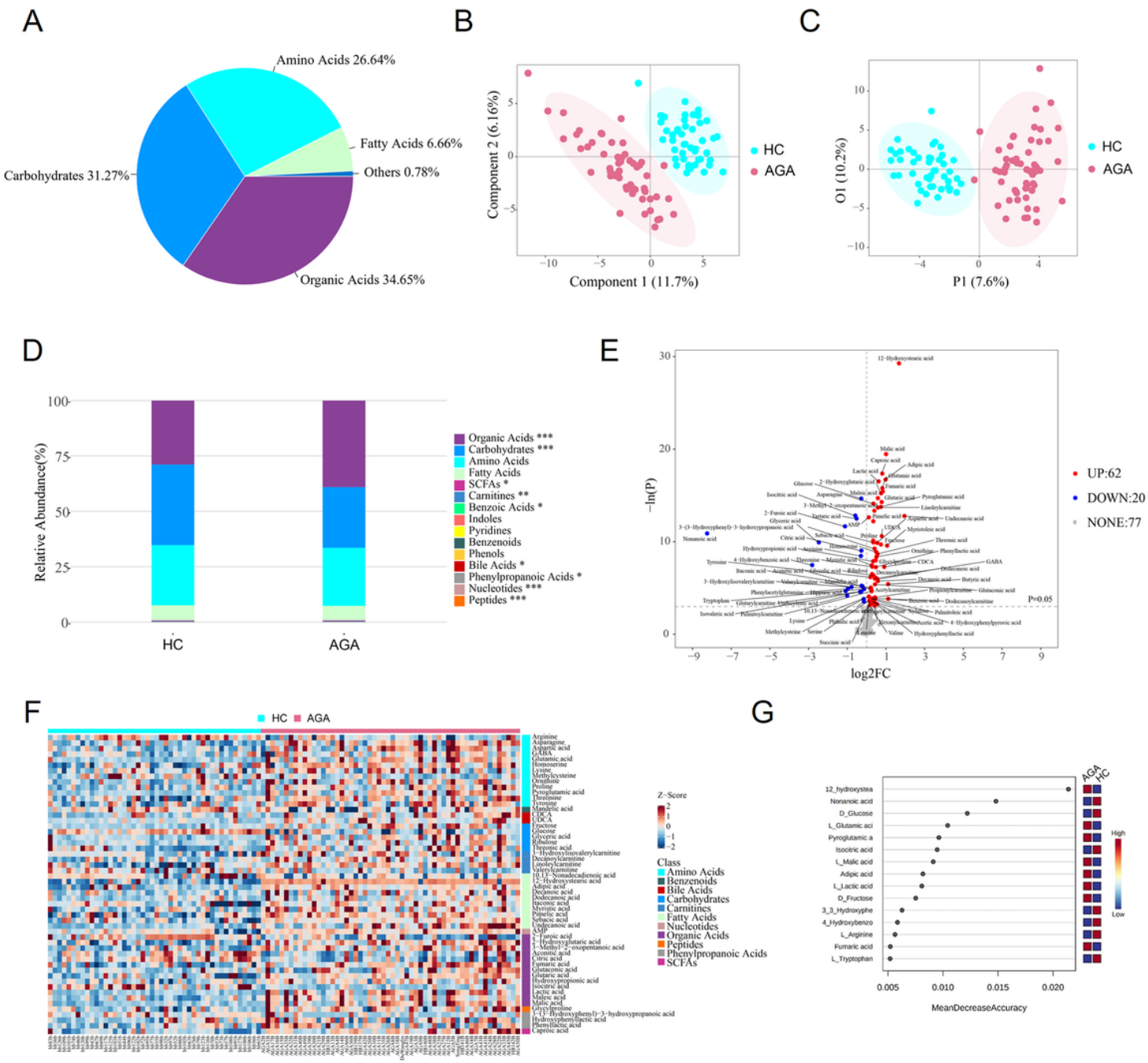

Figure 1

Serum metabolic profiling in patients with AGA identified by targeted metabolomics.

A The summary of detected metabolite counts in each metabolite class. **B** PLS-DA score plots from the healthy (n = 52) and AGA groups (n = 48). **C** OPLS-DA score plots from the healthy (n = 52) and AGA groups (n = 48). **D** The relative abundance of each metabolite classes in different groups is shown in the stacked bar chart. **E** Volcano plots of the identified metabolites. Each metabolite is plotted based on its

log2 FC in abundance (AGA/HC) and its −log10 P value in significance. The dashed horizontal line indicates P= 0.05. The red dots denote significantly upregulated metabolites, the blue dots denote significantly downregulated metabolites and the red dots denote metabolites with insignificant differences. **F** Visualization of 54 serum differential metabolite expression values in 2 groups by heatmap. G Random forest variable prediction of biomarkers. HC, healthy control (green)(n=52); AGA, androgenic alopecia patients (red)(n=48); SCFAs, short chain fatty acids. *P<0.05, **P<0.01, ***P<0.001, determined by two-tailed unpaired Student's *t*-test.

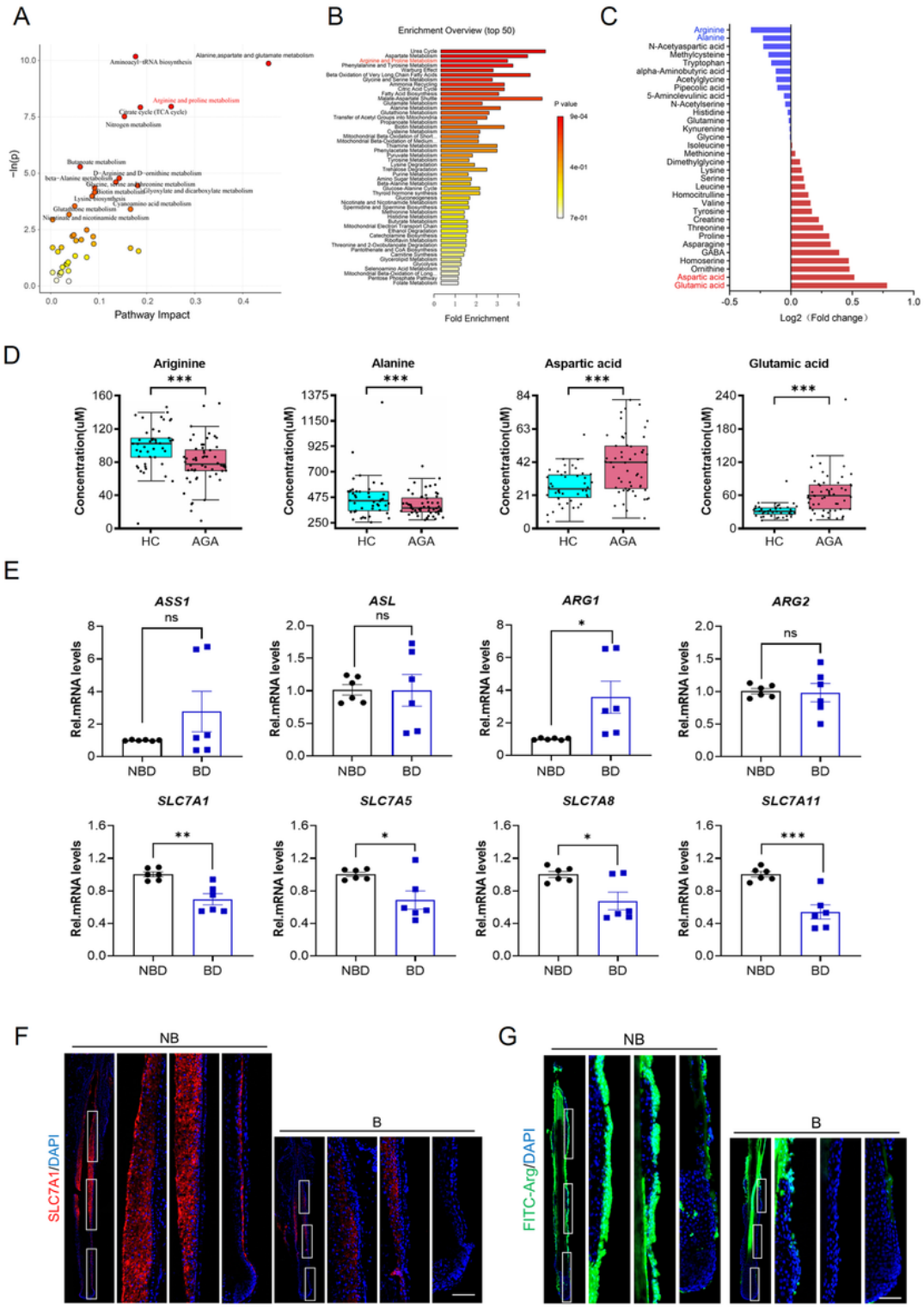

Figure 2

Arginine metabolism was aberrant in AGA patients.

A Pathway analysis bubble plot by hsa set using identified differential metabolites. **B**A diagram showing the MSEA of the identified metabolites. Red horizontal bars summarize the most significantly altered metabolic pathways. **C** Expression changes of the top 32 differential metabolites in amino acids. **D** Box plot of top 4 differential metabolites of arginine, alanine, aspartic acid, and glutamic acid metabolism pathway. HC, healthy control (green) (n = 52); AGA, androgenic alopecia patients (red) (n = 48). **E** Differential mRNA expression analysis of arginine synthetases, hydrolases and transporters in HFs from non-balding (NB) and balding (B) scalps of AGA patients (n=6). **F** Immunofluorescent staining of SLC7A1 on anagen HF sections from NB/B scalps of AGA patients (n=5 HFs from 3 patients). **G** Fluorescence images showing the uptake of FITC-Arg in anagen HFs from B and NB scalps of patients with AGA. Data information: Box plots show the interquartile range (box), median (line), and minimum and maximum (whiskers). The data represent the means ± SEM, *P<0.05, **P<0.01, ***P<0.001, determined by two-tailed unpaired Student's *t*-test. Scale bar, 50 μm. ASS1: argininosuccinate synthetase 1, ASL: argininosuccinate lyase, ARG1: arginase 1, ARG2: arginase 2, SLC7A1/5/8/11: solute carrier family 7 member 1/5/8/11.

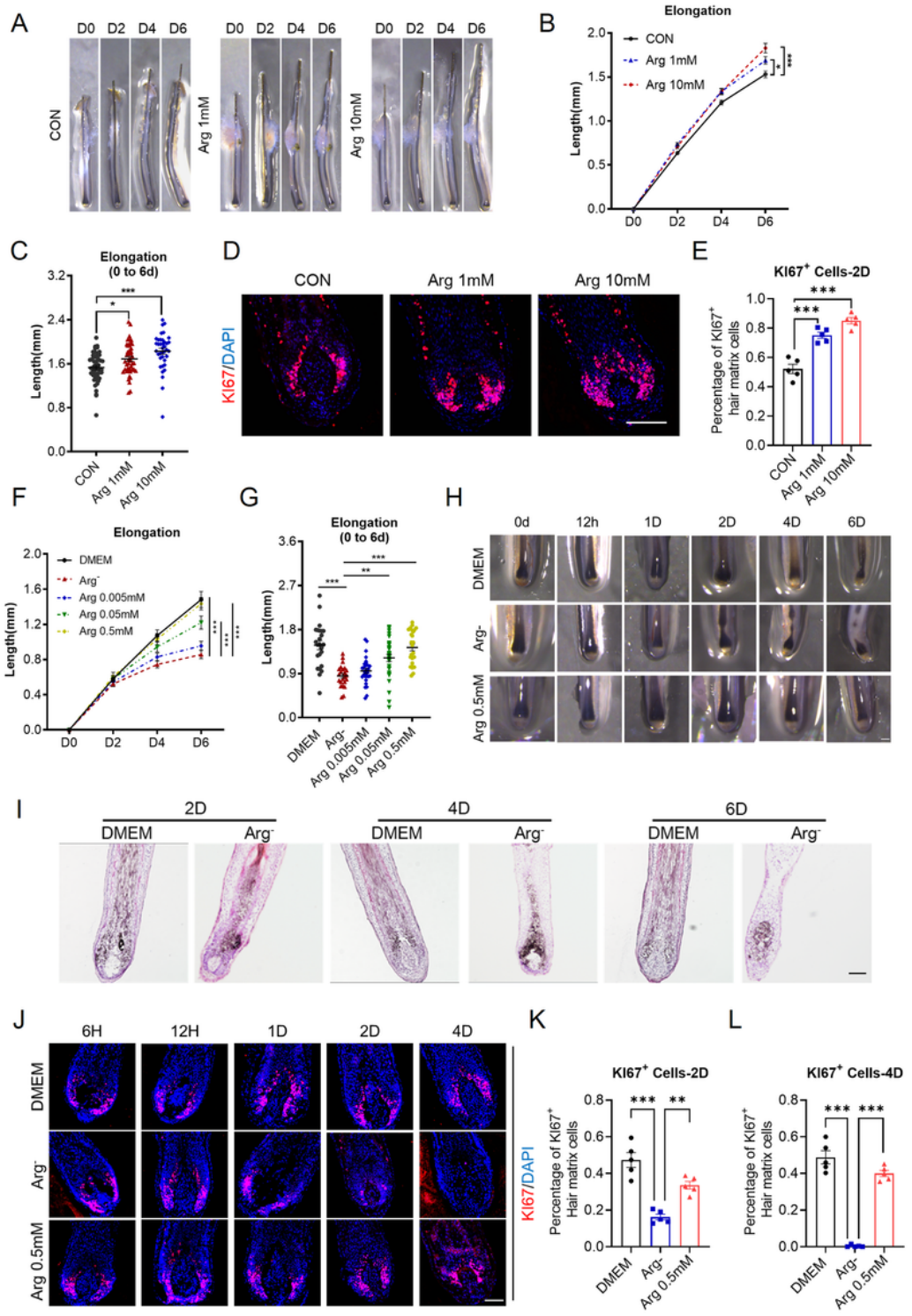

Figure 3

Arginine is essential for hair follicle growth ex vivo

A Representative images of hair shaft elongation of human HFs ex vivo with vehicle (CON) or arginine treatment at concentration of 1 mM and 10 mM (n=38-48 HFs from 3 donors for each group. The same individuals' HF samples were used in the following analysis and staining of HFs with the same

treatments). **B, C** The elongated length of the hair shaft (n=48/45/38). **D** Immunostaining of Ki67 on HF sections with indicated treatments on day 2. **E** Quantification of the percentage of $Ki67^+$ matrix cells. **F, G** The elongated length of the hair follicles culture in DMEM, medium with arginine deprivation (Arg^-) or Arg^- medium with arginine replenishment at concentration of 0.005 mM, 0.05 mM, 0.5 mM. (n=24/23/29/31/25 HFs from 3 donors for each group. The same individuals' HF samples were used in the following analysis and staining of HFs with the same treatments). **H** Representative images of the lower bulb of HFs culture in medium of DMEM/Arg^-/Arg^- with arginine replenishment at concentration of 0.5 mM on 0 h, 12 h and day 1/2/4/6. **I** H&E staining of the HFs with indicated treatments on day 2. **J** Ki67 staining of the HFs with indicated treatments on 0 h, 12 h and day 1/2/4. (n = 5 HFs for each group). **K, L** The quantification of the percentage of $Ki67^+$ matrix cells on day 2/4. The data represent the means ± SEM, *P<0.05, **P<0.01, ***P<0.001, determined by one-way ANOVA with Tukey's post hoc test (C, E, G, K, L) and two-way ANOVA with a post hoc Dunnett's multiple comparisons test (B, F). Scale bar: 50 μm.

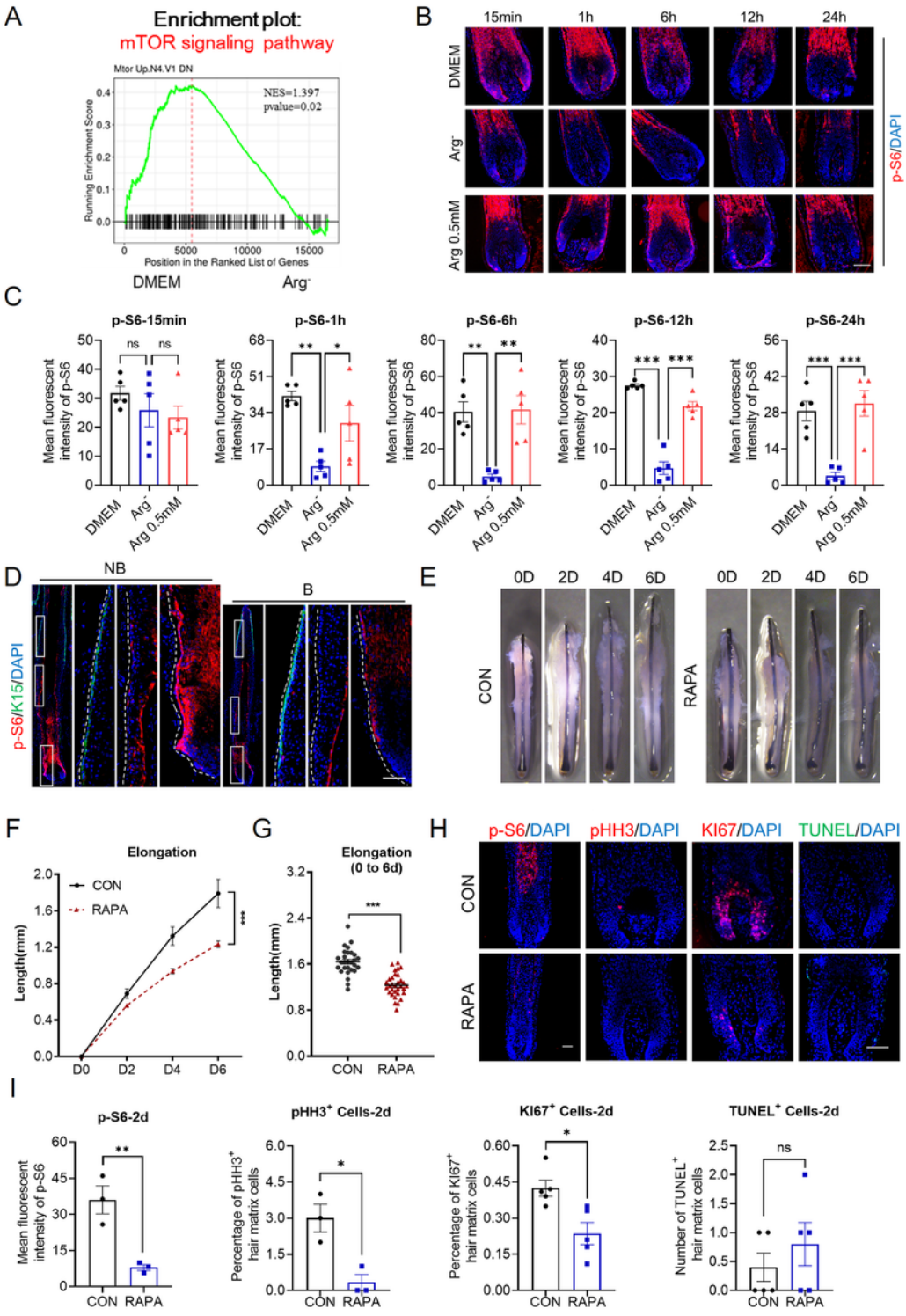

Figure 4

The mTOR signaling pathway in HFs was significantly inhibited under the condition of arginine deficiency.

A Enrichment curve showing enrichment of the mTOR signaling pathway in normal hair bulbs compared with hair bulbs treated with arginine deprivation. NES = 1.397; p.adj = 0.02. **B** Immunostaining of p-S6 on

HF sections treated with DMEM, arginine deprivation or arginine replenishment at concentration of 0.5 mM at different time points (15 min, 1 h, 6 h, 12 h and 24 h). (n = 5 HFs for each group). **C** The quantification of the mean fluorescent intensity of p-S6 on HF sections with indicated treatments. **D** Coimmunostaining of p-S6 and K15 on HF sections from B and NB scalps of patients with AGA. (n = 3 HFs for each group). **E** Typical images of the HFs treated with vehicle (CON) or RAPA (50 μM) on day 0/2/4/6. RAPA: rapamycin. (n = 24-31 HFs from 3 donors for each group. The same individuals' HF samples were used in the following analysis and staining of HFs with the same treatments). **F, G** The elongated length of the HFs with indicated treatments. (n = 28/31/26/24). **H** Immunostaining of p-S6, pHH3 and Ki67 and TUNEL staining on HF sections with indicated treatments on day 2. **I** The mean fluorescent intensity of p-S6, PHH3 and Ki67 and the number of $TUNEL^+$ matrix cells on HF sections with indicated treatments on day 2. (n = 5 HFs for each group). The data represent the means ± SEM, *P < 0.05, **P < 0.01, ***P < 0.001, determined by one-way ANOVA with Tukey's post hoc test (C, F, I) and two-way ANOVA with a post hoc Dunnett's multiple comparisons test (F). Scale bar, 100 μm.

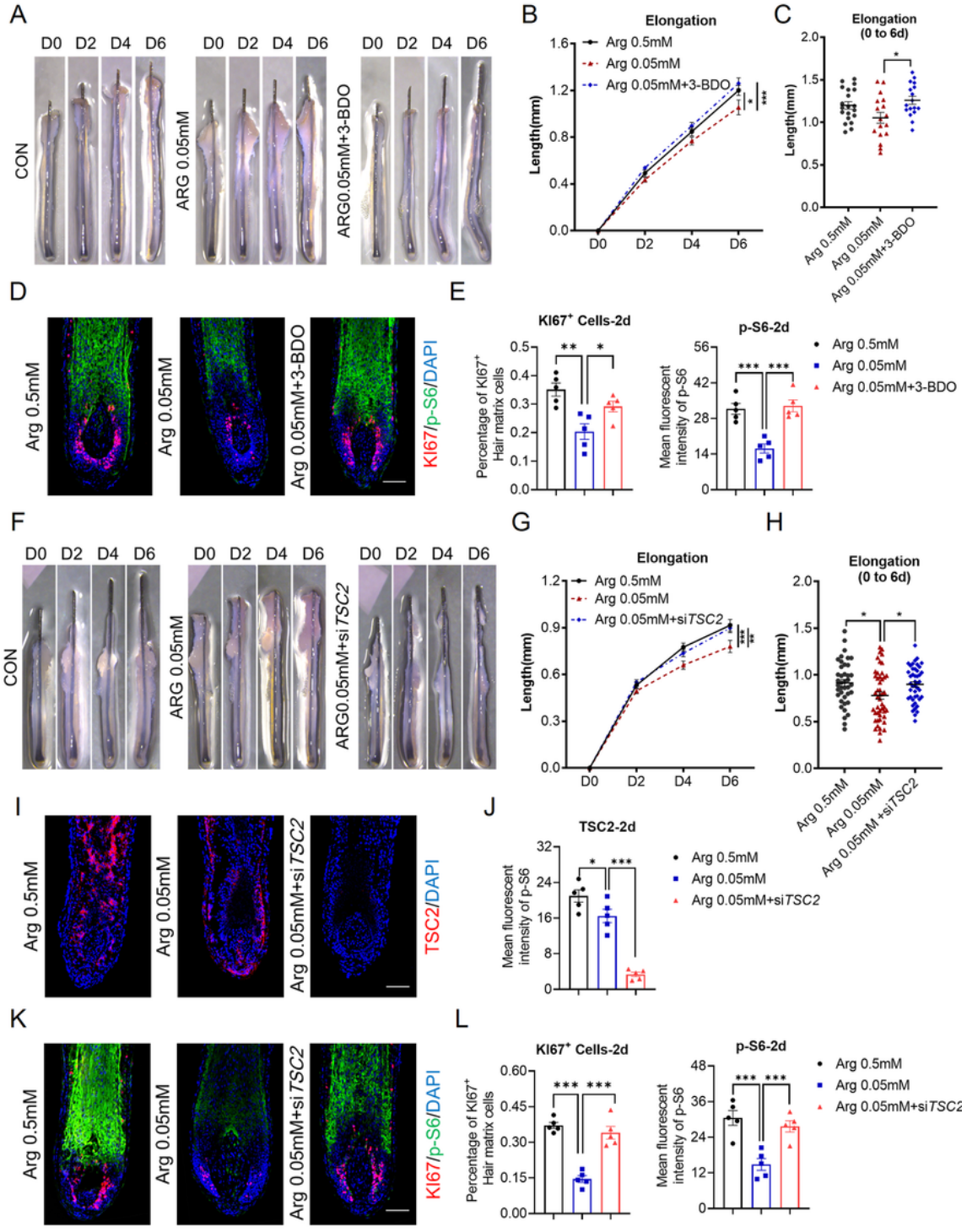

Figure 5

The growth-inhibiting effect of arginine deficiency on HFs was reversed by activation of the mTOR pathway.

A Representative images of the HFs treated with normal HF complete medium (CON), arginine deprivation (to 0.05 mM) or 3-BDO (5 μM) supplemention based on arginine deprivation on day 0/2/4/6. 3-BDO: a

mTOR signaling pathway agonist. (n = 17-20 HFs from 3 donors for each group. The same individuals' HF samples were used in the following analysis and staining of HFs with the same treatments). **B, C** The elongated length of the HFs with indicated treatments. (n = 20/17/17). **D** Coimmunostaining of p-S6 and Ki67 on HF sections with indicated treatments on day 2. **E** The quantification of the percentage of $Ki67^+$ matrix cells and the mean fluorescent intensity of p-S6 on HF sections with indicated treatments on day 2. (n = 5 HFs for each group). **F** Typical images of the hair follicles treated with arginine deprivation (to 0.05 mM) or siTSC2 interference based on arginine deprivation on day 0/2/4/6. (n = 40-47 HFs from 3 donors for each group. The same individuals' HF samples were used in the following analysis and staining of HFs with the same treatments). **G, H** The elongated length of the HFs with indicated treatments. (n = 40/47/44). **I** Immunostaining of TSC2 on HF sections with indicated treatments on day 2. (n = 5 HFs for each group). **J** The mean fluorescent intensity of TSC2 on HF sections with indicated treatments on day 2. **K** Coimmunostaining of p-S6 and Ki67 on HF sections with indicated treatments on day 2. (n = 5 HFs for each group). **L** The quantification of the percentage of $Ki67^+$ matrix cells and the mean fluorescent intensity of p-S6 on HF sections with indicated treatments on day 2. The data represent the means ± SEM, *P < 0.05, **P < 0.01, ***P < 0.001, determined by determined by one-way ANOVA with Sidak's (C, E,H,L,J) and two-way ANOVA with a post hoc Tukey's multiple comparisons test (B, G). Scale bar, 50 μm.

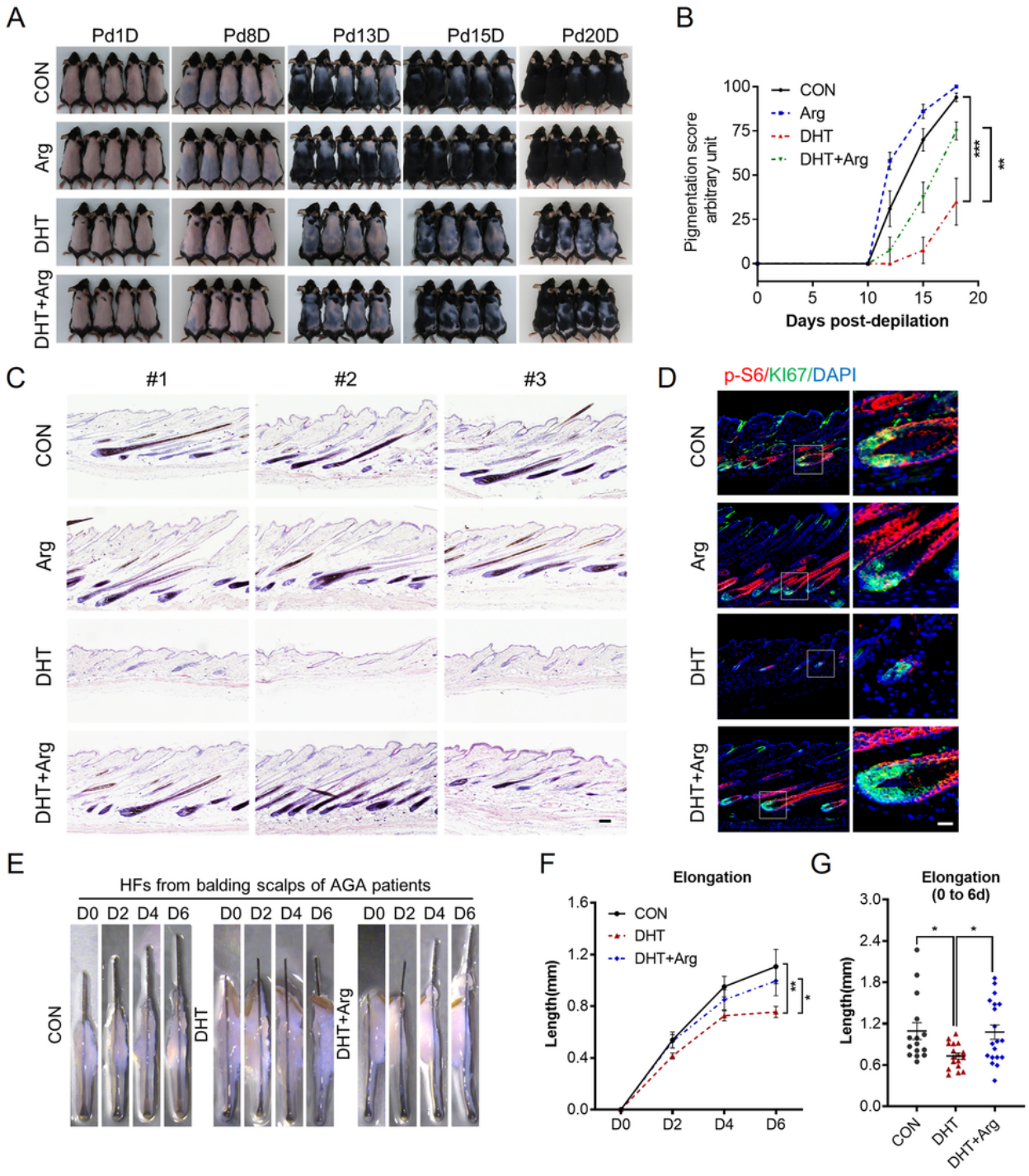

Figure 6

Arginine restored hair growth in AGA-like mice and HFs from AGA patients.

AThe hair coats of mice treated with L-arginine in their drinking water combined with subcutaneous DHT injection. Images were captured on Pd1D, Pd8D, Pd13D, Pd15D and Pd20D. Pd: post depilation. (n = 5/5/4/4). **B** The hair coat recovery score (described in Materials and Methods) after the back hair of mice

was shaved. **C** H&E staining of the back skin of mice in the indicated treatment groups at Pd15D. (n = 3 mice for each group). **D** Coimmunostaining of p-S6 and Ki67 of the back skin sections of mice in the indicated treatment groups at Pd15D. 3 mice for each group. **E** Typical images of the HFs treated with vehicle (CON), DHT (1 μM) or arginine (0.5 mM) combined with DHT on day 0/2/4/6. HFs were from balding scalps of AGA patients. (n = 15-20 HFs from 3 donors for each group. The same individuals' HF samples were used in the following analysis and staining of HFs with the same treatments). **F, G** The elongated length of the hair follicles with indicated treatments. (n = 15/17/19).

Supplementary Files

This is a list of supplementary files associated with this preprint. Click to download.

- FigureS1.tif
- FigureS2.tif
- FigureS3.tif
- FigureS4.tif
- FigureS5.tif
- FigureS6.tif
- SuppFigLegends.docx